An unbiased approach elucidates variation in (*S*)-(+)-linalool, a context-specific mediator of a tri-trophic interaction in wild tobacco

Jun He[a], Richard A. Fandino[b], Rayko Halitschke[a], Katrin Luck[c], Tobias G. Köllner[c], Mark H. Murdock[a,d,1], Rishav Ray[a], Klaus Gase[a], Markus Knaden[b], Ian T. Baldwin[a,2], and Meredith C. Schuman[a,e,2]

[a]Department of Molecular Ecology, Max Planck Institute for Chemical Ecology, 07745 Jena, Germany; [b]Department of Evolutionary Neuroethology, Max Planck Institute for Chemical Ecology, 07745 Jena, Germany; [c]Department of Biochemistry, Max Planck Institute for Chemical Ecology, 07745 Jena, Germany; [d]College of Life Sciences, Brigham Young University, Provo, UT 84606; and [e]Department of Geography, University of Zurich, 8057 Zürich, Switzerland

Edited by John G. Hildebrand, University of Arizona, Tucson, AZ, and approved June 4, 2019 (received for review October 29, 2018)

Plant volatile organic compounds (VOCs) mediate many interactions, and the function of common VOCs is especially likely to depend on ecological context. We used a genetic mapping population of wild tobacco, *Nicotiana attenuata*, originating from a cross of 2 natural accessions from Arizona and Utah, separated by the Grand Canyon, to dissect genetic variation controlling VOCs. Herbivory-induced leaf terpenoid emissions varied substantially, while green leaf volatile emissions were similar. In a field experiment, only emissions of linalool, a common VOC, correlated significantly with predation of the herbivore *Manduca sexta* by native predators. Using quantitative trait locus mapping and genome mining, we identified an (*S*)-(+)-linalool synthase (*NaLIS*). Genome resequencing, gene cloning, and activity assays revealed that the presence/absence of a 766-bp sequence in *NaLIS* underlies the variation of linalool emissions in 26 natural accessions. We manipulated linalool emissions and composition by ectopically expressing linalool synthases for both enantiomers, (*S*)-(+)- and (*R*)-(−)-linalool, reported to oppositely affect *M. sexta* oviposition, in the Arizona and Utah accessions. We used these lines to test ovipositing moths in increasingly complex environments. The enantiomers had opposite effects on oviposition preference, but the magnitude of the effect depended strongly both on plant genetic background, and complexity of the bioassay environment. Our study reveals that the emission of linalool, a common VOC, differs by orders-of-magnitude among geographically interspersed conspecific plants due to allelic variation in a linalool synthase, and that the response of a specialist herbivore to linalool depends on enantiomer, plant genotype, and environmental complexity.

Nicotiana attenuata | *Manduca sexta* | enantiomer-specific linalool synthase | tri-trophic interactions | oviposition preference

Plants use a variety of volatile organic compounds (VOCs) to mediate interactions with other organisms. VOC emissions from different tissues, such as leaves, flowers, fruit, and roots help to attract pollinators and seed dispersers, or defend against abiotic or biotic stress, including that from heat, ozone, herbivores, and pathogens (1, 2). However, herbivores also use plant VOCs as host location cues and feeding stimulants (1, 2). Two ubiquitous groups of plant VOCs are green leaf volatiles (GLVs) and terpenoids. GLVs comprise C_6 aldehydes, alcohols, and esters derived from fatty acids via the lipoxygenase (LOX)/hydroperoxide lyase (HPL) pathway, which are released upon damage from green tissues. The composition of GLV blends varies among plants and due to different causes of wounding (3–5). GLVs seem to be produced by all plants: the LOX/HPL pathway is also known from algae (6, 7). In contrast, while the general pathways of terpenoid biosynthesis are also conserved in higher plants (8), the production of specific terpenoid VOCs among the thousands of possible structures varies greatly from plant to plant (4, 9). Terpenoid VOCs include hemiterpenes (C_5), monoterpenes (C_{10}), sesquiterpenes (C_{15}), and a few diterpenes (C_{20}), and their derivatives, synthesized from the mevalonate (MVA) or the 2-C-methyl-D-erythritol 4-phosphate/1-deoxy-D-xylulose 5-phosphate (MEP/DOXP) pathway (10). Terpenoid VOCs directly synthesized by terpene synthases (TPSs) (8) are often emitted in response to stresses, and could have many functions in stress responses and interactions (11). Both GLVs and terpenoids have been shown to attract predators or parasitoids of herbivores, a phenomenon termed indirect defense, and some directly deter herbivore oviposition (12, 13). Considering the diverse interactions mediated by VOCs and their structural diversity, their functions may be highly specific. Interestingly, common VOCs, such as linalool, are also known to have multiple functions in different interaction systems (14).

Linalool is a monoterpenoid alcohol with 2 enantiomeric forms, (*R*)-(−)-linalool and (*S*)-(+)-linalool; both occur frequently in nature. In plants, linalool has been detected from many species (15). One plant species may produce only 1 enantiomer, but others can produce both enantiomers with dynamic composition, for example across individuals or development stages (16–18). Linalool has

Significance

The monoterpene alcohol linalool, occurring as 2 enantiomers, is made by many organisms and mediates diverse ecological interactions, including the attraction of both herbivores and their predators to plants. The specific effect of linalool differs by enantiomer and across interactions. Here, we used a forward genetics approach, which identified linalool as a candidate indirect defense compound produced by the wild tobacco *Nicotiana attenuata* against the specialist herbivore *Manduca sexta*. Linalool emission varied by orders-of-magnitude across 26 *N. attenuata* accessions, due to geographically interspersed allelic variation of a linalool synthase gene. We identified specific effects of the enantiomer, but also plant genotype and ecological context, which determined linalool's effect on *M. sexta* behavior within this plant–insect interaction.

Author contributions: J.H., R.A.F., R.H., T.G.K., K.G., M.K., I.T.B., and M.C.S. designed research; J.H., R.A.F., R.H., K.L., T.G.K., M.H.M., R.R., K.G., and M.C.S. performed research; R.R. and K.G. contributed new reagents/analytic tools; J.H., T.G.K., M.H.M., R.R., K.G., and M.K. analyzed data; and J.H., R.A.F., R.H., T.G.K., K.G., M.K., I.T.B., and M.C.S. wrote the paper.

The authors declare no conflict of interest.

This article is a PNAS Direct Submission.

Data deposition: The sequences reported in this paper have been deposited in the GenBank database (accession nos. LOC109240002 and LOC109235079). Source data are available at https://edmond.mpdl.mpg.de/imeji/collection/Kpsiw8PSKETsPdQV.

[1]Present address: Department of Surgery, University of Pittsburgh, Pittsburgh, PA 15213.

[2]To whom correspondence may be addressed. Email: Baldwin@ice.mpg.de or meredith.schuman@geo.uzh.ch.

This article contains supporting information online at www.pnas.org/lookup/suppl/doi:10.1073/pnas.1818585116/-/DCSupplemental.

Published online July 1, 2019.

been documented to have several functions in plants: as a common component of floral scent (15), it is correlated with pollinator attraction, especially for hawkmoths (19–22). Linalool emitted from *Datura wrightii* (angel's trumpet) flowers stimulates visiting and feeding by *Manduca sexta* (tobacco hornworm) moths and, interestingly, mated female moths were attracted only by (*S*)-(+)-linalool but repelled by (*R*)-(−)-linalool (23). However, in some cases floral linalool and its derivatives do not attract pollinators but function as repellents of floral antagonists (24). Linalool is also often found in foliar VOCs, especially in herbivory-induced plant volatiles. For example, linalool accumulates in the trichomes of *Solanum lycopersicum* cv. Moneymaker (tomato) leaves and stems and is induced by wounding, jasmonic acid application, and herbivory by *Tetranychus urticae* (red spider mites) (25). (*S*)-(+)-Linalool is the most abundant herbivory-induced VOC in *Oryza sativa* (rice) plants attacked by *Spodoptera frugiperda* (fall armyworm) larvae, and the application of synthetic racemic linalool to rice plants attracted *Cotesia marginiventris* parasitic wasps, which are also attracted to *S. frugiperda*-damaged plants (26, 27). Linalool was also found in herbivory-induced VOCs from *Vicia faba* (broad bean) plants damaged by *Acyrthosiphon pisum* (pea aphids) and was attractive to the aphid parasitoid *Aphidius ervi* in wind-tunnel assays (28). Linalool in insects may function as a pheromone (29) and an antipathogen defense compound (30), and has been reported in multiple bacteria and fungi where its functions have not been revealed (31). Because linalool is ubiquitous in the biosphere, with contrasting functions in different interaction systems, its role has been recognized as highly context-dependent (14). However, few studies have addressed the essential question of how context affects linalool function.

The wild tobacco *Nicotiana attenuata* has been established as an ecological model plant for which interactions with many insects in its native environment, including the specialist Lepidopteran pollinator and herbivore *M. sexta* and predatory *Geocoris* spp. (big-eyed bugs), have been well characterized. Previous studies showed that complex blends of terpenoids, including (*E*)-β-ocimene, linalool, and (*E*)-α-bergamotene, can be detected in the headspace of *N. attenuata* plants and that these compounds vary among natural accessions (9, 12). The addition of racemic linalool, but also (*E*)-α-bergamotene and several other herbivory-induced VOCs, to wild *N. attenuata* plants in a natural population in Utah (UT) significantly increased the predation of *M. sexta* eggs; linalool further decreased oviposition by adult moths (12). Two *N. attenuata* genotypes originating in Arizona (AZ) and Utah, which vary in many traits (32–34), were used to develop an advanced intercross recombinant inbred line (AI-RIL) population (34). With this population, the gene encoding the (*E*)-α-bergamotene synthase was mapped and characterized and this compound was found to function both in attracting *M. sexta* moths to pollinate flowers, and indirectly defending leaves from *M. sexta* larvae (34).

Here, we used an integrated approach to dissect natural variation in herbivory-induced foliar VOCs and their function in tritrophic interactions in *N. attenuata*. Field predation assays using the AI-RIL population derived from the AZ and UT accessions revealed that linalool is a key attractant for native predators in Arizona. Quantitative trait locus (QTL) mapping and genome mining, together with gene cloning and expression, was used to identify and characterize a linalool synthase gene, *NaLIS*. The *NaLIS* gene displayed allelic variation, which explained variation in linalool production among 26 *N. attenuata* accessions collected from a selection of habitats within the range of the species. Natural accessions and RILs produced only the (*S*)-(+)-linalool enantiomer, and we used ectopic expression of enantiomer-specific linalool synthase (LIS) genes to either enhance the production of (*S*)-(+)-linalool, or introduce foreign (*R*)-(−)-linalool into the AZ and UT *N. attenuata* accessions. Oviposition assays using mated *M. sexta* females in increasingly complex and realistic environments demonstrated that the enhancement of (*S*)-(+)-linalool and introduction of (*R*)-(−)-linalool affect the oviposition preference of *M. sexta* moths differently depending on the enantiomer and plant accession. Furthermore, we found that ectopic expression of these linalool enantiomers did not affect the growth of *M. sexta* larvae. Together, these results provide evidence for context-dependent functions of a ubiquitous VOC, linalool, and imply local selection operating on plant signals mediating tritrophic interactions.

Results

Terpenoid VOC Emissions Are Highly Variable in Natural Accessions and a Derived Genetic Mapping Population. The AZ and UT accessions differ in many traits, including the release of individual VOCs from leaves and flowers (32–34). Here, we show that the differences in leaf headspace composition are extensive and primarily due to differences in terpenoid VOCs. We detected 33 VOCs emitted by at least 1 accession after leaves were treated with wounding and application of *M. sexta* regurgitant (W+R). These compounds comprised 17 GLVs and 14 terpenoids, as well as nicotine and benzyl alcohol (Fig. 1*A* and *SI Appendix*, Fig. S1*A* and Table S1). While the release of GLVs was similar, most terpenoids were enriched in one or the other accession. Abundance of the monoterpenoids (*E*)-β-ocimene and linalool were 36- and 3.5-fold higher, respectively, in the AZ versus the UT headspace, while sesquiterpenoids—including (*E*)-α-bergamotene, α-farnesene, sesquiphellandrene, and 5 unidentified terpenoids—were much more abundant in the UT versus the AZ headspace (Fig. 1*A* and *SI Appendix*, Table S1). Only 2 terpenoids, α-duprezianene and an unidentified sesquiterpene (retention time 27.3 min), were similar in relative abundance in the 2 accessions.

We further profiled foliar VOCs from plants in an AI-RIL population generated from crossing Arizona and Utah (34), after leaves were treated by W+R. Variation of terpenoid emissions among the 261 RILs was large and extended beyond the differences between the parental accessions (Fig. 1*B* and *SI Appendix*, Fig. S1*B*). For example, the range of (*E*)-α-bergamotene and linalool emission was 522- and 115-fold in the AI-RILs, compared with a 38- and 3.5-fold difference in the parents, respectively. Across the 261 RILs, the relative amount of (*E*)-α-bergamotene in the leaf headspace was correlated with the relative amount of (*E*)-β-ocimene, but not linalool (Fig. 1*B*).

Among Variable Leaf VOCs, Linalool Is Correlated with Predation Rates of *M. sexta* by Native Predators in the Field. We selected 6 RILs with large differences in terpenoid composition for a field predation assay. These RILs represented extremes in the emission of 6 terpenoids, including (*E*)-β-ocimene, α-farnesene, linalool, (*E*)-α-bergamotene, and 2 unknown sesquiterpenes with retention times of 22.8 and 23.8 min (*SI Appendix*, Fig. S1). The randomly distributed RILs and both parental lines were tested for predation rates of experimentally distributed *M. sexta* eggs and larvae. This experiment was conducted in a field plot at the Walnut Creek Center for Education and Research (WCCER) (Fig. 1*C*) near Prescott, Arizona. During the experimental period, we observed *Geocoris* spp. predators on several plants in the field and most of the predation occurred during the daytime, when *Geocoris* spp. are active (35). In total, predation rates on *M. sexta* eggs and larvae during the whole assay ranged from 3 to 19% (Fig. 1*C*). The predation rates on different genotypes were positively correlated with the relative abundance of linalool, but not of the 5 other terpenoids, which varied in the headspace of these lines (Fig. 1*D*).

Natural Variation of Linalool Is Driven by Allelic Variation in an Identified Linalool Synthase, *NaLIS*. We used QTL mapping and genome mining to determine the genetic components underlying

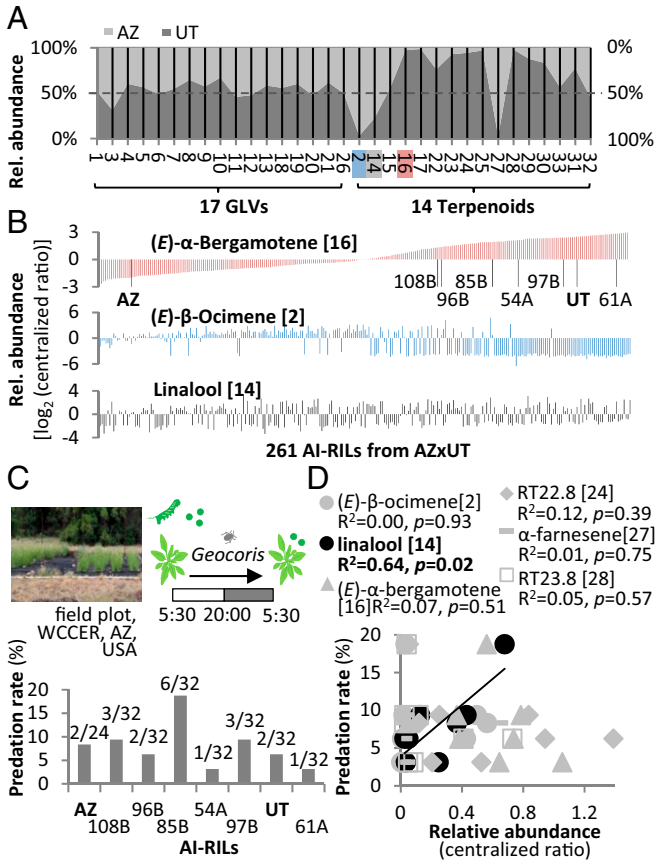

Fig. 1. *N. attenuata* accessions from Utah and Arizona differ in terpenoid emissions and among these, linalool is correlated with predation rates on *M. sexta*. (*A*) Relative abundance of VOCs in headspace of AZ and UT leaves. For each peak, the sum of the mean peak areas in AZ and UT, shown in *SI Appendix*, Table S1, is set to 100% (see *SI Appendix*, Table S1 for compound IDs). Boxed IDs indicate the compounds shown in *B*. (*B*) The distribution of relative abundances of (*E*)-α-bergamotene (34), (*E*)-β-ocimene, and linalool within the AI-RIL population. Numbers in brackets indicate the compound IDs (*SI Appendix*, Table S1). (*C*) Selected lines with large differences in terpenoid composition (*SI Appendix*, Fig. S1*B*) received different predation rates on *M. sexta* larvae and eggs in a field plot in Arizona. Numbers of predated larvae and eggs and numbers of total larvae and eggs placed on the plants are shown on top of the bars. The 2 parental lines are indicated by bold text. The assay lasted 72 h. Larvae and eggs were placed onto leaves at around 0500 hours and predated eggs and larvae were counted and supplemented at around 2000 hours. The following morning they were counted again and all larvae and eggs were replaced. Counting was repeated at dusk and the next morning. *Geocoris* spp. appeared in the field during the assay. Field plot image courtesy of R. Carlson (photographer). (*D*) Among 6 variable terpenoids, only linalool is correlated with predation rate across the assayed lines. Numbers in brackets indicate the compound IDs (*SI Appendix*, Table S1).

the variation of foliar VOCs in *N. attenuata* accessions. The published QTL for (*E*)-α-bergamotene was successfully reidentified in our dataset, with a higher LOD value than originally published (*SI Appendix*, Fig. S2) (34). In total, 8 terpenoids were mapped to the same locus or nearby loci (*SI Appendix*, Fig. S2). In contrast, a dominant single locus for linalool was mapped to a different linkage group (Fig. 2*A*). Because only the genome of UT has been well sequenced (36), we first analyzed the linalool locus in the UT genome. The corresponding region was located on the short arm of chromosome VIII, with a length of around 316 kb. In the parallel region of the *S. lycopersicum* genome, there are 4 putative *TPS* genes (*SI Appendix*, Fig. S3). However, NIATv7_g00838 is the only *TPS* at this region in the *N. attenuata* genome and no other genes share collinearity with the *SlTPS*s. We further mined data for the whole *NaTPS* family in *N. attenuata* (sequences in Dataset S1, and see refs. 37, 38). Aligning the sequences of all putative *TPS* genes, we found that the putative CDS of NIATv7_g00838 (later confirmed by sequencing) could be classified as a single member of the subclade *TPS*-g (*SI Appendix*, Fig. S4), possibly encoding a linalool/nerolidol synthase. NIATv7_g00838 was later renamed *NaLIS*.

Using the *Nicotiana attenuata* Data Hub (http://nadh.ice.mpg.de/NaDH/) (39), we found that the transcript abundance of *NaLIS* was relatively high in leaves, and present at lower levels in some floral organs, such as anthers and the stigma, ovary, and pedicel, but not detectable in the corolla or calyx. This is in agreement with the fact that linalool is abundant as a foliar VOC in some accessions, but not detected in floral VOCs of *N. attenuata* (*SI Appendix*, Fig. S5*A*). Using qPCR, we found the transcript abundance of *NaLIS* was strongly correlated with the amount of internal extractable linalool in leaves of transgenic plants in the UT background [ir*MPK4* (40), which emits greater amounts of most VOCs (*SI Appendix*, Table S2) and empty vector (EV) controls] for plants under different treatments, including light deprivation or abscisic acid treatment (Fig. 2*C* and *SI Appendix*, Fig. S5). Additionally, we identified 2 genes putatively encoding geranyl diphosphate (GPP) synthase (responsible for biosynthesis of the monoterpenoid substrate GPP), one of which was also highly correlated with the abundance of internal linalool (*SI Appendix*, Fig. S5), indicating coregulation of *NaLIS* and *NaGPPS2*.

NaLIS displays allelic variation between AZ and UT, both in the genomic DNA and cDNA. Alignment of the genome region bearing *NaLIS* in AZ and UT (sequences in Dataset S1) showed that a 766-bp sequence is present in AZ but missing in UT (Fig. 2*D*). Comparing putative transcripts of *NaLIS*-AZ and *NaLIS*-UT to reported homologous genes in relatives such as *S. lycopersicum*, *Solanum tuberosum*, and *Nicotiana tomentosiformis* revealed that *NaLIS*-AZ has a similar *TPS* exon–intron structure to these relatives, while *NaLIS*-UT does not. *NaLIS*-AZ has 6 exons and 5 introns. The missing sequence of *NaLIS*-UT is part of intron 5 and exon 6. Leaf transcriptome data (http://nadh.ice.mpg.de/NaDH/) from the 2 accessions revealed that the remnant sequence of intron 5 and exon 6 of *NaLIS*-UT was still transcribed, but the right border of exon 5 (left border of intron 5) was not spliced. Therefore, the *NaLIS*-UT transcript was 168-bp longer than *NaLIS*-AZ. However, we identified an in-frame TAG stop codon transcribed from intron 5 in the *NaLIS*-UT transcript. This resulted in the ORF of *NaLIS*-UT not only lacking exon 6 (278 bp) of *NaLIS*-AZ, but also including a 110-bp sequence from intron 5, and thus the full-length CDS is 168-bp shorter than that of *NaLIS*-AZ. Based on the different genome and transcriptome information, we designed primers and amplified the full-length ORFs of both *NaLIS*-AZ and *NaLIS*-UT from cDNA prepared from leaves of AZ and UT, respectively (Fig. 2*E*). Sequencing of the amplicons confirmed the expected sequence variation in the *NaLIS* alleles from AZ and UT.

We tested the activities of the 2 *NaLIS* variants in vitro (Fig. 2*F*). The putative plastid-targeting signal peptide was truncated and the remaining sequence from each allele was heterologously expressed in *Escherichia coli*. The extracted enzymes showed different activities depending on the terpenoid precursor supplied. When GPP was used as substrate, NaLIS-AZ produced approximately 10-fold as much linalool as NaLIS-UT under identical assay conditions (Fig. 2*F*). NaLIS-AZ also produced nerolidol from (*E*,*E*)-farnesyl diphosphate (FPP) and geranyllinalool from (*E*,*E*,*E*)-geranylgeranyl diphosphate (GGPP), whereas NaLIS-UT did not produce detectable terpenoids from these 2 precursors (*SI Appendix*, Fig. S6). The full-length protein of NaLIS-AZ showed similar activity as the truncated protein when expressed in *E. coli*, but with lower efficiency, while the full-length protein of NaLIS-UT did not convert any of the substrates in the in vitro assay.

ECOLOGY

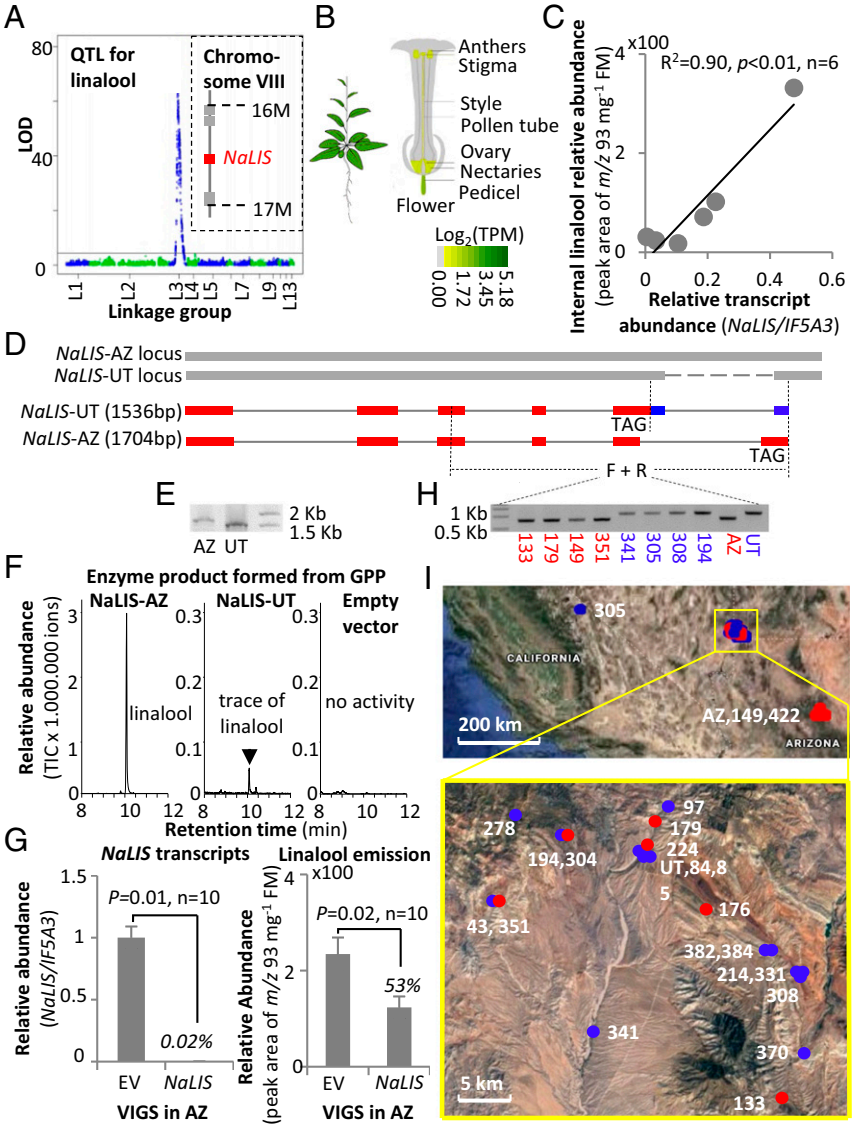

Fig. 2. *NaLIS* underlies variation in linalool emission among *N. attenuata* accessions. (*A*) A single QTL was mapped for linalool using the AI-RIL population and a single TPS was found within the mapped locus. The putative *TPS* gene is shown as a red bar, other proximate genes in gray. (*B*) *NaLIS* in the UT accession is constitutively expressed in leaves, and in some floral tissues (no data are available for stem and root tissue). The relative transcript abundance of *NaLIS* among different tissues was extracted from the *N. attenuata* Data Hub (http://nadh.ice.mpg.de/NaDH/) (39). TPM, transcripts per million. (*C*) In transgenic plants of the UT background (ir*MPK4*, which emits greater amounts of most VOCs, and EV controls), abundance of internal free linalool extracted from leaves is highly correlated with relative transcript abundance of *NaLIS* under different treatments shown in *SI Appendix*, Fig. S5 (mean + SE, $n = 3$). *IF5A3* was used as reference gene. (*D*) Alignment of the *NaLIS* genome region and different transcripts in AZ and UT shows splicing variation between the 2 accessions at the last exon of the gene. Gray bars represent sequences of the *NaLIS* genome locus. The dashed line represents a sequence of 766 bp missing in the UT genome compared with AZ. Red bars indicate exons of *NaLIS* in UT and AZ. Blue bars indicate transcribed sequence after the stop codon (TAG) in UT. *NaLIS*-UT has a longer transcript that includes a 110-bp sequence on the fifth exon, which is present in the intron region of the AZ variant (and also homologous genes in other relative species including tomato, potato, and *N. tomentosiformis*). A stop codon at the end of this 110-bp sequence makes the ORF of *NaLIS*-UT smaller than that of *NaLIS*-AZ. The sequence information on the transcripts of *NaLIS*-UT and *NaLIS*-AZ was extracted from the *N. attenuata* Data Hub (http://nadh.ice.mpg.de/NaDH/) (39) and later confirmed by cloning and sequencing. (*E*) ORFs of *NaLIS*-AZ and *NaLIS*-UT amplified from cDNA of the 2 accessions. (*F*) Heterologously expressed *NaLIS* ORFs produce linalool from GPP. NaLIS-AZ has much higher activity than NaLIS-UT in paralleled assays (note difference in scales of *y* axes). NaLIS-AZ can also accept (*E*,*E*)-FPP and (*E*,*E*,*E*)-GGPP to produce nerolidol and geranyllinalool, respectively, as shown in *SI Appendix*, Fig. S6. (*G*) VIGS of *NaLIS* in AZ caused reduced emission of linalool from leaves (mean + SE, $n = 10$). AZ was used here because it has higher emission of linalool as shown in Fig. 1*A* and a more active NaLIS. Relative abundance of transcript: *NaLIS/IF5A3*, relative abundance of linalool: peak area of *m/z* 93 mg^{-1} FM. (*H*) Amplified different 3′ ends of *NaLIS* in 10 natural accessions. The *NaLIS*-UT variant is correlated with nondetectable or extremely low linalool emissions (peak area of *m/z* 93 mg^{-1} FM < 30 counts/s in measurements, accession ID in blue) and the *NaLIS*-AZ variant is correlated with high linalool emission (peak area of *m/z* 93 mg^{-1} FM > 300 counts/s in measurements, accession in red). For relative abundance of linalool sampled in the headspace of these accessions, see *SI Appendix*, Fig. S7. (*I*) Geographic distribution of 26 natural accessions (including the 10 shown in *H*) and their linalool emission. Dots in blue indicate where the low linalool accessions were collected, and dots in red indicate where the high linalool accessions were collected from *N. attenuata*'s native range. For relative abundance of the linalool emission, *NaLIS* alleles and transcript accumulation in these accessions see *SI Appendix*, Fig. S7. Satellite images courtesy of Google Earth.

Subsequently, the activity of *NaLIS* was studied in vivo. We inserted a 205-bp gene-specific sequence of *NaLIS*-AZ into the pTV00 vector in an antisense orientation, and used the resulting construct for virus-induced gene silencing (VIGS) in AZ plants. VIGs nearly eliminated transcripts of *NaLIS* and significantly decreased the emission of linalool from W+R-treated leaves compared with control plants, which were infiltrated with an EV control (Fig. 2*G*); residual linalool emission may be due to existing levels of NaLIS protein before VIGS took effect, but see the discussion of linalool conjugates in *Discussion*.

Linalool is also highly variable among 24 other natural accessions of *N. attenuata* collected from different parts of *N. attenuata*'s native range, in addition to Arizona and Utah (*SI Appendix*, Fig. S7*A*). We classified 16 of these 26 accessions as low-linalool emitters (peak area of *m/z* 93 mg^{-1} FM < 30 counts/s) and 9 accessions as high-linalool emitters (peak area of *m/z* 93 mg^{-1} FM > 300 counts/s) based on linalool emission from W+R-treated leaves. Between the highest of the low emitters, accession 331, and the lowest of the high emitters, accession 179, there is a 19-fold difference, indicating a qualitative difference separating the low- and high-emitter groups. In contrast, the highest linalool emitter, accession 133, only emitted approximately 11-fold as much linalool as accession 179. We selected 4 accessions from each category and analyzed the length of *NaLIS* transcripts at the 3′ end. The 4 low-emitting accessions produce the UT variant of *NaLIS*, while the 4 high-emitting accessions produce the AZ variant of the *NaLIS* transcript (Fig. 2*H*).

We mapped the reads to chromosome VIII carrying *NaLIS* and manually assembled the genomic sequence of *NaLIS* for the 26 accessions (sequences in Dataset S1, and see refs. 37, 38). All of the high linalool emitters had the functional *NaLIS*-AZ allele, while all low linalool emitters had the deletion on intron 5 and exon 6 of the gene (*SI Appendix*, Fig. S7*B*). In contrast to the tight correlation with the allelic variation, the linalool emission did not correlate with *NaLIS* transcript abundance assayed by RNA-seq across the 26 accessions (*SI Appendix*, Fig. S7*C*).

The analyzed accessions were collected from different locations in the natural range of *N. attenuata* (Fig. 2*I*). The greatest distance between collection sites was 696 km between California (low-linalool emitter 305) and Arizona (high-linalool emitters AZ, 149 and 422). The remaining accessions, including 4 low-linalool emitters and 3 high-linalool emitters, were from a region covering approximately 448 km^2 near the border between Utah and Nevada. These accessions are all less than 33.5 km from each other, where high- and low-linalool emitters were interspersed (Fig. 2*I*).

Expressing Foreign *LIS* Genes in *N. attenuata* Plants Alters Emission of the Endogenous Enantiomer (*S*)-(+)-Linalool or the Foreign Enantiomer (*R*)-(−)-Linalool. There are 2 natural enantiomers of linalool, and both occur in plants and are reported to be perceived differently and elicit different behavioral responses in *M. sexta* (23, 41, 42). We analyzed W+R-induced foliar VOC samples from Arizona, Utah, and 50 RILs, along with racemic linalool, a pure (*R*)-(−)-linalool standard and enzyme products of NaLIS-AZ from (*E*,*E*)-FPP using a chiral GC column. Only (*S*)-(+)-linalool was detected in the NaLIS-AZ products and in all of the tested *N. attenuata* genotypes (Fig. 3*A*).

We altered the enantiomer-specific linalool production in *N. attenuata* plants via ectopic expression of 2 foreign *LIS* genes, *CbLIS*, from *Clarkia breweri* for (*S*)-(+)-linalool and *ObLIS* from *Ocimum basilicum* for (*R*)-(−)-linalool (42, 44). Each *LIS* under control of the CaMV35 promoter was separately introduced into AZ and UT plants, respectively, resulting in 4 different types of ectopic expression lines (Fig. 3*B*). AZ-(*S*) and UT-(*S*) lines are AZ or UT plants expressing *CbLIS*, which enhances emission of (*S*)-(+)-linalool, while AZ-(*R*) and UT-(*R*) lines express *ObLIS* in the AZ or UT background and emit (*R*)-(−)-linalool, which is absent in *N. attenuata* WT accessions. We subsequently screened transgenic lines for diploidy and homozygosity of transgene insertions, and used T2 plants of each line. We then measured linalool emission from unelicited plants, because we aimed to select plants for *M. sexta* oviposition assays (see below), and many W+R-induced VOCs have been shown to reduce *M. sexta* oviposition (12); moths lay only one or a few eggs per *N. attenuata* plant (12, 45) and seem to avoid plants already damaged by conspecifics.

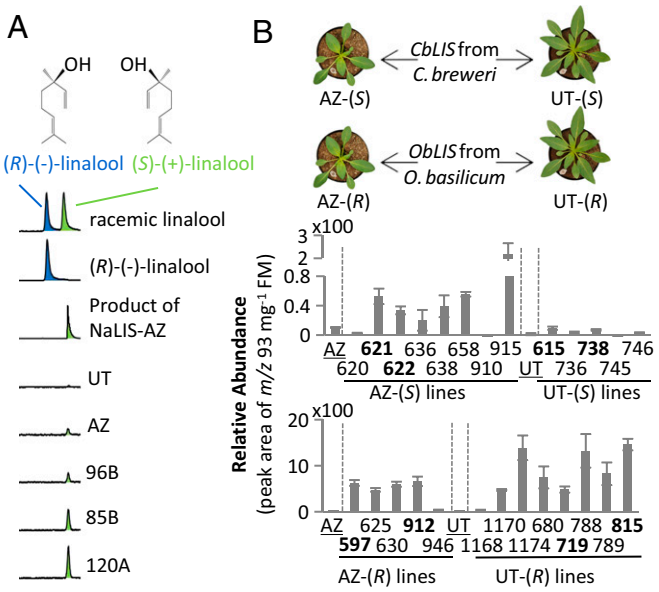

Fig. 3. Enantiomer identification of linalool produced in *N. attenuata* and linalool emission from transgenic plants with ectopic overexpression of different linalool enantiomer synthase genes. (*A*) Chromatogram for racemic linalool, standard (*R*)-(−)-linalool, major enzyme product of NaLIS-AZ from (*E*,*E*)-FPP, and linalool produced by UT, AZ, and 3 of 50 tested RILs. No (*R*)-(−)-linalool was found in any tested WT lines. (*B*) Profile of linalool in AZ and UT WT plants and in different ectopic expression lines expressing either *CbLIS* from *C. breweri* (produces (*S*)-(+)-linalool) or *ObLIS* from *O. basilicum* (produces (*R*)-(−)-linalool) in either the AZ or UT background (mean + SE, n = 3). Numbers in bold indicate the lines selected for further study. Shown here are the sum of 2 enantiomers measured using a standard nonpolar GC column. Different enantiomers were identified later in representative lines using a chiral column. In UT-(*S*) and AZ-(*S*) lines only (*S*)-(+)-linalool was found. In UT-(*R*) lines only (*R*)-(−)-linalool was found. Both enantiomers were detected in AZ-(*R*) lines; the ratios of the 2 enantiomers in the selected lines are shown at the top of the bars. Data from WT plants are from an independent experiment and are shown for comparison. Notice the different scales in every chart. Photo of *C. breweri* is from Wikipedia, by Eric in SF; *O. basilicum* picture: J.H.; *N. attenuata* images courtesy of A. Kügler (photographer).

We found that the ectopic lines as well as the corresponding WT genotypes emitted linalool constitutively (Fig. 3). The (*S*)-linalool emission from ectopic lines was within the range of natural variation among accessions of *N. attenuata* (*SI Appendix*, Fig. S9 and Dataset S2). Of 8 AZ-(*S*) lines, 6 emitted significantly more linalool than AZ WT plants, with increases ranging from 1.9- to 21.3-fold. Of 5 UT-(*S*) lines, 3 emitted 2.4- to 7.3-fold higher linalool levels than UT WT plants. Five AZ-(*R*) lines emitted 3.7- to 64.4-fold as much total linalool as AZ WT, while linalool emissions from 8 UT-(*R*) lines were 18.9- to 1,149.3-fold higher than the UT WT emission. While AZ-(*S*) lines produced on average 18-fold higher linalool emissions than the corresponding UT-(*S*) lines, the release of linalool was on average 1.8-fold higher in UT-(*R*) compared with AZ-(*R*) lines. Besides the differences in linalool emissions, other terpenoid VOCs measured from these ectopic expression lines were similar to the corresponding WT plants (*SI Appendix*, Fig. S8 and Dataset S3; lines used for further experiments are highlighted in *SI Appendix*). None of the transgenic lines except AZ-915(*S*) showed any

ECOLOGY

morphological or developmental differences from germination to the flowering stage, and line AZ-915(*S*) was not used in further experiments.

Enantiomer-specific linalool production was verified in representative ectopic expression lines using a chiral GC column. Only (*S*)-(+)-linalool was found in UT-(*S*) and AZ-(*S*) lines and only (*R*)-(−)-linalool was found in UT-(*R*). Both enantiomers were detected in AZ-(*R*) lines, with (*S*)-(+)-linalool only 0.3% as abundant as the (*R*)-(−)-linalool isomer (Fig. 3*B*).

Based on linalool emission, we selected 2 lines of each background–foreign gene combination (Fig. 3*B*) for further study. Among the 8 selected lines, UT-738(*S*) and UT-719(*R*) were confirmed to have a single insertion of T-DNA using Southern blotting by hybridizing an hptII probe to genomic DNA digested with XbaI or EcoRI (*SI Appendix*, Fig. S10*A*). For the remaining 6 selected lines, a single and complete T-DNA insertion was demonstrated using NanoString's nCounter technology. Multiple probes (sequences in Dataset S1) with different fluorescent barcodes were hybridized to sheared genomic DNA of each line to be tested, and scanned and counted in an nCounter Sprint instrument. Hybridization of 5 probes designed from transgene promotor (P_{NOS}, P_{35S}) and terminator (T_{NOS}, T_{35S}), as well as the selective marker gene (*hptII*) sequences indicated a single and complete insertion of the transformation cassette in all 6 lines (*SI Appendix*, Fig. S10*B*). Moreover, 2 probes designed from the transformation vector backbone outside the right and left transfer borders (nptII, pVS1) showed that only 3 lines harbor T-DNA overreads, which did not affect the transgenic phenotype or stability of inheritance. Very little background signal was observed for the 2 hybridization probes (nptIII, sat-1) designed from sequences not present on the pSOL9*CbLIS*/*ObLIS* plasmids (*SI Appendix*, Fig. S10*B*). Transgenic lines screened in this study are listed in *SI Appendix*, Table S2.

Linalool emissions from natural accessions of *N. attenuata* show a diurnal rhythm, with higher emissions during daytime and low emissions at nighttime (9). In the UT accession used in our experiments, linalool was emitted in greater abundance from W+R-treated leaves during the day, and this was light-dependent (*SI Appendix*, Fig. S11*A*). In the transgenic plants, both enantiomers followed a similar rhythm with greater emissions during day than night (*SI Appendix*, Fig. S11*B*). However, there were still considerable amounts of linalool of both enantiomers detected in the headspace during the dusk and night periods when *M. sexta* moths are active. This allowed us to compare behavioral responses to the specific linalool enantiomers, which are perceived differently by *M. sexta* adults (23, 41, 42).

Enhancement of Linalool Enantiomers in *N. attenuata* Leaves Alters Oviposition Preferences of *M. sexta* in an Accession-Specific Manner. We tested the oviposition preference of mated female *M. sexta* moths for AZ and UT WT plants versus transgenic plants with altered linalool emissions. Thus, AZ and UT WT plants and 4 ectopic expression lines—AZ-621(*S*), AZ-597(*R*), UT-738(*S*), and UT-1174(*R*)—were used to assay oviposition by *M. sexta* moths. Assays were conducted in 3 increasingly complex and realistic environments (Fig. 4). Because these ectopic expression plants constitutively emit linalool, and many *M. sexta*-elicited VOCs have been shown to deter *M. sexta* moth oviposition (12), we used unelicited plants for these assays.

First, binary choice assays were performed in a wind tunnel, where the input air was filtered through activated charcoal to remove background odors and wind speed and directions were strictly regulated. For each trial, a single mated female moth was released downwind of the plant pair in the tunnel during a standardized time window in which moths are known to actively oviposit, and allowed to choose between paired plants of AZ WT and UT WT, or an ectopic expression line and the corresponding WT. The moth was observed for the first 10 touches (any part of the moth body contacting the plant) and then removed; the order

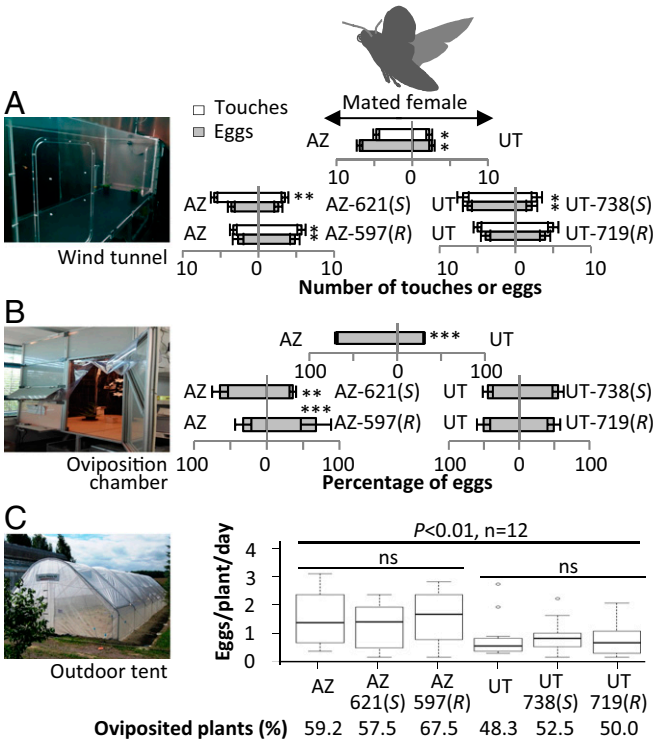

Fig. 4. Ectopic expression of (*S*)-(+)-linalool and (*R*)-(−)-linalool in UT and AZ accessions differently affect oviposition preference of mated female *M. sexta* moths. (*A*) First 10 touches of moths and the corresponding eggs laid on plants in binary choice assays in a wind tunnel (mean + SE, sign tests; $*P < 0.05$; $**P < 0.01$, $***P < 0.001$, $n = 20$). Wind tunnel picture: R.A.F. (*B*) Percentage of eggs laid on plants overnight in a climate chamber. Asterisks (*) indicate statistically significant differences (mean + SE, sign tests; $*P < 0.05$; $**P < 0.01$, $n = 20$). Oviposition chamber picture: J.H. (*C*) Eggs oviposited per plant per night by 1 single mated female moth in the tent. (Friedman tests for overall difference, Tukey–Kramer multiple comparison tests for comparisons of interest, $P < 0.05$, $n = 12$). Percentages of plants of each type receiving at least 1 egg (summed across all assays) are shown below the plot. Tent image courtesy of D. Kessler (photographer).

and number of visitations and the corresponding number of eggs laid on each plant were recorded (Fig. 4*A*). AZ WT plants, which have higher (*S*)-(+)-linalool emission, were touched more often and received more eggs than UT WT plants. However, compared with AZ WT plants, the (*S*)-(+)-linalool-enhanced AZ-621(*S*) were touched significantly fewer times, and tended to receive fewer eggs ($P = 0.18$). Similarly, UT-738(*S*) plants were touched fewer times and received fewer eggs than UT WT. In contrast, (*R*)-(−)-linalool–emitting AZ-597(*R*) plants were visited more often than AZ WT plants and received more eggs, while UT-1174(*R*) was visited and received a similar number of eggs as the UT WT. In all assays, the numbers of touches on each plant were correlated to the number of eggs oviposited.

We subsequently tested the same binary combinations of lines in a free-flying climate chamber where a colony of moths could oviposit overnight on plants of paired genotypes (Fig. 4*B*). In the chamber, air was not filtered and airflow was not controlled. Similar to the results from wind-tunnel assays, more eggs were oviposited on AZ WT than on UT WT in this more complex environment. AZ-621(*S*) received fewer, and AZ-597(*R*) received more eggs than AZ WT, respectively. However, neither UT-738(*S*) nor UT-1174(*R*) received significantly different numbers of eggs compared with UT WT plants.

Finally, all 4 ectopic expression lines and both WTs were tested simultaneously in a large outdoor tent, which represented a semi-

natural environment (Fig. 4*C*). In the tent, 10 plants of each genotype (60 plants in total) were placed at random positions at standardized distances (1.5 m from each other). A single newly mated moth was released into the tent and kept overnight for oviposition. Of a total of 16 moths tested, 12 oviposited at least 20 viable eggs in the trials. In this environment, ovipositing moths generally preferred WT and transgenic plants of the AZ background (Friedman tests, $P < 0.01$, $n = 12$). AZ-621(*S*) tended to receive fewer eggs than AZ WT and AZ-597(*R*). However, no significant difference was found between any ectopic expression line and the corresponding WT plants (Tukey–Kramer multiple comparisons tests). We also noticed that for each genotype, more than 48% of the plants received at least 1 egg, indicating high oviposition activity by the moths. Among all 6 genotypes, AZ-597(*R*) had the highest proportion of plants receiving eggs (Fig. 4*C*).

Linalool-Derived Glycosides Covary with Emitted Linalool and Do Not Affect Growth of *M. sexta* Larvae. A large proportion of linalool produced in plants is converted to different derivatives or conjugated and stored in tissues rather than emitted to the headspace, and these conjugates have different functions in plant interactions (24, 46, 47). The most abundant linalool conjugates found in plant tissues are linalool glucosides, from which linalool can be released by glucosidase treatment (48). Similar to the headspace linalool emission, the linalool glycoside levels also varied in W+R-treated leaves of natural *N. attenuata* accessions (*SI Appendix*, Fig. S12*A*). Furthermore, the amount of glucosidase-released linalool from W+R-induced leaves was strongly correlated with the linalool emission from W+R-elicited leaves in these accessions (*SI Appendix*, Fig. S12*B*). In contrast to the foliar headspace containing only (*S*)-(+)-linalool, the glucosidase treatment released more 8-hydroxylinalool (*SI Appendix*, Fig. S12*C*) in addition to linalool. We identified additional linalool derivatives by comparison of leaf extracts from unelicited leaves of AZ WT, AZ-621(*S*), and AZ-912(*R*) using UPLC-HR-MS/MS. Several metabolites were increased in the ectopic expression lines compared with WT plants. The strongest difference was observed in a putative hydroxylinalool hexose conjugate ($C_{16}H_{28}O_7$) (*SI Appendix*, Fig. S11*D*). The accumulation of this compound showed a similar pattern as the emitted linalool in the 3 genotypes. Furthermore, this compound was also detected in the frass of *M. sexta* larvae when fed on these plants. The concentration of this compound in larval frass was correlated with its abundance in the leaf tissue of the food plant.

In no-choice bioassays, we therefore tested whether ectopic expression of linalool enantiomers influenced the growth of *M. sexta* larvae. Freshly hatched *M. sexta* larvae were allowed to feed on hydrated, cut leaves from AZ WT, AZ-621(*S*), and AZ-912(*R*) plants. After 7 d of feeding larval mass did not significantly differ between larvae grown on WT control plants and plants with altered (*S*)-(+)- or (*R*)-(−)-linalool accumulation.

Discussion

The 2 *N. attenuata* accessions from Arizona and Utah vary in multiple physiological traits and differ in many biological functions (32–34). In this study we compared the foliar headspace of the 2 accessions, and found the most variable VOCs to be terpenoids (Fig. 1 *A* and *B*). Among the variable terpenoids, linalool was the only compound correlated with rates of herbivore mortality due to native predators in a field plot in Arizona (Fig. 1*C*). By profiling the foliar headspace of an AZ × UT AI-RIL population and conducting QTL analysis (34), we identified and characterized the *NaLIS* gene, which is responsible for the biosynthesis of linalool in *N. attenuata* plants (Fig. 2 *A*–*G*). Allelic variation in this gene corresponded to variation in linalool emission across 26 *N. attenuata* accessions from geographically interspersed locations (Fig. 2 *H* and *I*). We identified the linalool enantiomer produced in *N. attenuata* to be (*S*)-(+)-linalool and tested its function by either enhancing the emission of this enantiomer or introducing the foreign (*R*)-(−)-linalool enantiomer, in both the AZ and UT backgrounds, by ectopically expressing 2 foreign enantiomer-specific *LIS* genes (Fig. 3). We found that supplementing linalool emission affected the oviposition choice of *M. sexta* female moths on *N. attenuata* plants in an enantiomer- and accession-specific manner (Fig. 4). Although the ectopic expression lines also accumulated greater amounts of nonvolatile linalool conjugates, the growth rate of *M. sexta* larvae was similar on leaves from the ectopic expression lines and WT plants. Our study demonstrates the importance of context in determining functions of linalool even within a single plant–insect interaction, and indicates specific aspects of context that may be important.

Linalool Varies Independently of Other Terpenoid VOCs in *N. attenuata*. Several terpenoid VOCs, including (*E*)-β-ocimene, (*E*)-α-bergamotene, and linalool varied strongly between the *N. attenuata* AZ and UT accessions (Fig. 1 *A* and *B*). Except for linalool, all other variable terpenoid VOCs were mapped to the same single QTL, which was previously identified for (*E*)-α-bergamotene using the AI-RIL population (*SI Appendix*, Fig. S2) (34). Thus, the results of our genetic analysis are consistent with the observation that *TPS*s are often clustered in plant genomes (8). In contrast, our mapping analysis identified a strong QTL for linalool emissions (Fig. 2*A*) on a linkage group different from the previously identified TPS cluster locus (Fig. 2*A* and *SI Appendix*, Fig. S3) (34). Therefore, the linalool synthase may be free to evolve and segregate independently of other terpenoid VOCs for which the genes are linked. The interspersed geographic distribution of the *N. attenuata* accessions with different levels of linalool emission provides evidence that selection for linalool is local and occurs on small scales, not clearly separated by geographic features (Fig. 2*I*).

Allelic variation of *NaLIS* is a determinant, but not the only factor, shaping the variation of linalool emission in *N. attenuata*. Between accessions, *NaLIS* alleles determined low or high linalool emission independently of transcript abundance (Fig. 2 *D*, *H*, and *I* and *SI Appendix*, Fig. S7), while in 23 of the 26 accessions examined in this study, the transcript levels of TPS38 strongly correlated with the emission of (*E*)-α-bergamotene in both flowers and herbivore-induced leaves (34). However, within the UT background, transcript abundance of *NaLIS* corresponded to tissue-specific differences in linalool emission (Fig. 2*B*), and for transgenic plants subjected to different treatments, linalool emission covaried with transcript abundance of *NaLIS* (*SI Appendix*, Fig. S5). Furthermore, reduction in transcript abundance using VIGS also reduced linalool emission in the AZ background (Fig. 2*G*). These data indicate that transcript abundance of *NaLIS* determines linalool emission within a genotype. Interestingly, even ectopic expression lines, which produce foreign LIS genes under the control of the constitutively active CamV 35S promoter, showed variation in headspace linalool abundance at different times of day (*SI Appendix*, Fig. S10), suggesting that substrate availability may be an additional important factor, as was previously indicated for (*E*)-α-bergamotene and (*E*)-β-farnesene emissions in *N. attenuata* (49). Consistent with this observation, a monoterpenoid substrate synthase gene, *NaGPPS2*, was found coregulated with *NaLIS* transcription and linalool emission (*SI Appendix*, Fig. S5*D*).

Although linalool is variable among *N. attenuata* accessions, NaLIS belongs to a clade of TPSs relatively conserved in enzymatic function. We identified NaLIS to be the single member of the TPS-g clade in the NaTPS family (*SI Appendix*, Fig. S4). In plants, the TPS-g clade is angiosperm-specific and well-known to produce acyclic monoterpenes (8, 50). TPS-g is usually a small clade compared with the highly divergent TPS-a and TPS-b clades. The single member of TPS-g in *Arabidopsis thaliana*, At1g61680, was found to contribute to floral (*S*)-(+)-linalool

emission and to produce nerolidol in vitro (51). Similarly, TPS-g members, which are (*S*)-(+)-linalool/nerolidol synthases, have been found in *Fragaria* × *ananassa* cv Elsanta (52), *O. sativa* (27), *S. lycopersicum* (53), and *Gossypium hirsitum* (54). However, TPS-g proteins in *Antirrhinum majus* were also found to produce (*E*)-β-ocimene and myrcene (50). In contrast to the presence of 2 functional linalool/nerolidol synthases and 2 mutants in the *S. lycopersicum* genome, NaLIS was the only ortholog identified in the *N. attenuata* genome (*SI Appendix*, Fig. S4). Moreover, more than half of the 26 *N. attenuata* accessions studied bore the less-efficient UT allele, in which exon 6 has been lost and a 110-bp redundant sequence has been fused to exon 5 (Fig. 2*D* and *SI Appendix*, Fig. S7*B*). This allele generally seems to have reduced enzymatic efficiency, and its activity toward FPP and GGPP seem to be abolished; but it can still convert GPP to linalool, suggesting that differences between the *N. attenuata* alleles may be involved in determining substrate specificity versus promiscuity of LIS enzymes.

Linalool Enantiomers Alter a Single Tritrophic Interaction in a Context-Dependent Manner. Linalool has been identified in more than 200 plant species. It is a common floral fragrance and has been long considered as a pollinator attractant (22, 23, 55). However, linalool emissions have also been reported to function in plant defense to repel florivores and other antagonistic flower visitors (24, 56, 57). Studies using linalool application, or genetic modification of linalool emission by ectopic expression or silencing of LIS genes, have shown that foliar linalool can mediate interactions between plants and herbivores. For example, racemic linalool has been reported to attract *Geocoris pallens* predators and deter *Manduca quinquemaculata* oviposition in a field study of a wild *N. attenuata* population (12); to repel *Myzus persicae* aphids from *A. thaliana* (46); to deter *Helicoverpa armigera* oviposition on *Nicotiana tabacum* (54, 58); and to influence choice of multiple herbivores, predators, and parasitoids on *O. sativa* (59). Thus, it is generally accepted that linalool mediates different outcomes depending on the interaction system. However, the way that context exerts influence is poorly understood, and different contexts are usually not directly compared, and assumed not to be relevant within the bounds of a single interaction.

In the present study, we selectively enhanced enantiomers of linalool in *N. attenuata* accessions with highly differentiated VOC backgrounds (Figs. 1*A* and 3). This enabled us to investigate the accession-specific effects of linalool enantiomers on *M. sexta* moth oviposition behaviors. Previous reports showed that supplementation of *Datura wrightii* flowers with (*S*)-(+)-linalool alone or in mixture with other floral VOCs increased oviposition rates by *M. sexta* moths, while addition of (*R*)-(−)-linalool reduced oviposition compared with control plants (23). In our study, AZ plants, which naturally produce (*S*)-(+)-linalool from leaves, received more oviposition from *M. sexta* moths, but enhancement of (*S*)-(+)-linalool by ectopic expression decreased oviposition (Fig. 4). Moreover, supplementation of (*S*)-(+)-linalool in the UT background by ectopic expression repelled *M. sexta* females in a wind-tunnel binary choice assay (Fig. 4*A*), but had no effect in the more complex environments of oviposition chambers shared by several moths (Fig. 4*B*), or an outdoor tent in which all genotypes were available for a single moth (Fig. 4*C*). The (*R*)-(−)-linalool enantiomer showed accession-specific effects on *M. sexta* preference: it increased oviposition in the AZ background, but had no effect in the UT background even though the UT ectopic expression lines emitted larger amounts of (*R*)-(−)-linalool (Figs. 3 and 4). These results indicate that moths use linalool as a context-specific cue, not only in the context of different plant species and tissues, but also depending on different characteristics, such as leaf VOC profile within a plant species. Moth decisions about oviposition are driven by a combinatorial olfactory code (60): that is, by taking into account not only the neuronal response to linalool but at the same time the activation of multiple olfactory receptors responding to other relevant GLVs and terpenoids. In addition to linalool, other terpenoids, such as (*E*)-α-bergamotene and (*E*)-β-ocimene, were also highly variable among the *N. attenuata* accessions (Fig. 1 *A* and *B*) and thus we could choose individuals representing the extremes of different VOCs (*SI Appendix*, Fig. S1*B*). Foliar (*E*)-α-bergamotene in *N. attenuata* reduces survivorship of *Manduca* spp. eggs (12), while floral (*E*)-α-bergamotene can attract *M. sexta* moths for pollination (34). The effects of other terpenoids in this system are less well understood. How linalool interacts with other VOCs and plant characteristics to influence the behavior of *M. sexta* moths requires further investigation. However, the context-dependent effects of linalool enantiomers on gravid female *M. sexta*, combined with the very local difference in linalool emission and, presumably, selective pressures, are consistent with the geographic mosaic theory of coevolution (61).

The different biological functions of linalool enantiomers in plant interactions are supported by the different perception of these 2 enantiomers by animals. Linalool enantiomers can be distinguished by the human nose and have different odor thresholds (62). They also evoke different neural responses in insects. However, context-defined functions of each linalool enantiomer are not well understood, but have been suggested by some studies on neural responses of *M. sexta* to linalool or linalool mixed with other compounds contained in *D. wrightii* floral VOCs (21), which showed that the neural ensemble evoked by the single compound did not resemble those evoked by mixtures. By testing the glomeruli activities in *M. sexta's* antennal lobe evoked by 80 odors separately, Bisch-Knaden et al. (42) showed that both (*S*)-(+)-linalool and (*R*)-(−)-linalool, as well as racemic linalool, evoked stronger and more broadly distributed activity in glomeruli compared with other terpenoid compounds. Furthermore, both enantiomers individually, and the racemic mixture, induced feeding behavior of *M. sexta* moths. In contrast, none of the 3 VOCs alone elicited oviposition behaviors, although both enantiomers strongly stimulated activities in multiple oviposition-related glomeruli (42).

Linalool has also been reported to mediate plant indirect defense by attracting predators and parasitoids of herbivores (59, 63, 64). In this study we showed that emission of linalool in different *N. attenuata* RILs is correlated with predation of eggs and larvae of *M. sexta* by natural enemies in a natural habitat (Fig. 1 *C* and *D*). It is possible that the avoidance of *M. sexta* females of linalool in certain *N. attenuata* accessions is, at least in part, the result of variable selection pressure from predators in nature.

Conjugation of Linalool in *N. attenuata*. Linalool is known to be metabolized to nonvolatile derivatives. For example, overexpression of *CbLIS* in petunia yielded nearly no emitted linalool but abundant accumulation of linalolyl-β-D-glucopyranoside (48), and *A. thaliana* expressing *FaNES1* produced more hydroxylated or glycosylated linalool derivatives than free linalool (46). Expressing *FaNES1* in *Chrysanthemum morifolium* produced, in addition to volatile linalool, 4 nonvolatile linalool glycosides, including 2 putative linalool-malonyl-hexoses, a linalool-pentose-hexose, and a glycoside of hydroxy-linalool (47). Two cytochrome P450s (CYP71B31 and CYP76C3) were coexpressed with 2 linalool synthases (TPS10 and TPS14) in flowers of *A. thaliana* and converted linalool enantiomers into hydroxylated or epoxidized products (17).

In our study, β-glucosidase treatment released approximately 200 times as much linalool from the *N. attenuata* leaf as was measured in the headspace of accessions (*SI Appendix*, Fig. S12*A*), and the natural conjugate pool of linalool was strongly correlated with headspace linalool (*SI Appendix*, Fig. S12*B*). The linalool conjugates may act as direct defenses against herbivory. Engineering linalool emission in chrysanthemum by expressing *FaNES* attracted *Frankliniella occidentalis*, but the increased abundance of linalool conjugates in tissues was repellent (47). When

the major linalool metabolizing oxygenase CYP76C3 was knocked out in *Arabidopsis*, the plant became more attractive to floral antagonists, including *F. occidentalis*, *Spodoptera littoralis*, *Plutella xylostella*, and *Phaedon cochleariae* (24). However, in our study, the growth of *M. sexta* larvae on leaf tissue was not affected by the ectopic expression of either the native or the foreign linalool enantiomer (*SI Appendix*, Fig. S12*F*). Furthermore, linalool conjugates are still abundant in the frass of *M. sexta* larvae and thus seem generally not to be metabolized after ingestion by larvae (*SI Appendix*, Fig. S12*E*). This indicates that the altered oviposition preferences of *M. sexta* moths are not due to an alteration of plants' nutritional quality: linalool seems to be more important as a signal in the interaction between *N. attenuata* and *M. sexta*. It is possible that under certain conditions, linalool could be released from the conjugate pool because in the VIGS experiment linalool emission was only reduced to half, while *NaLIS* transcripts were reduced by 99.8% (Fig. 2*G*). However, because VIGS is induced in rosette-stage plants, it is also possible that some amount of NaLIS protein was produced in the leaves we measured, before VIGS took effect. VIGs experiments were also conducted in climate chambers, where levels of background contamination may be higher than in a glasshouse or field.

Conclusion

Our data indicate that the ecological function of the ubiquitous biological VOC linalool depends both on the enantiomer and on details of the interaction context that can vary within species on a small scale. This is in contrast to previous studies, which have focused on context-dependence across different species and interactions. Our study reveals important factors for understanding the evolution and functions of VOC-mediated signaling in plant–insect interactions. For example, our data indicate that other specific VOCs may determine the response of *M. sexta* moths to the same enantiomer of linalool produced by different genotypes of the same plant species. The active VOCs might be revealed by series assays with different mixtures of linalool and various coemitted VOCs, or the expression or suppression of different GLVs and terpenoids, together with linalool enhancement/reduction in *N. attenuata* accessions, could be used to test linalool's context-dependent function.

Materials and Methods

The description of plant and animal materials, cultivation, plant treatment, headspace sampling, metabolite analyses, genetic, genomic, and transcriptional analyses, gene cloning and heterologous expression, moth oviposition, and larval growth assays, all based on published procedures, are detailed in *SI Appendix*. As the predation assay motivated our focus on linalool, and because this is a report of the nCounter method for transgene copy number and insertion integrity, those methods are presented here. All sequence data are provided in Dataset S1 or public databases, as described below. Source data are available at https://edmond.mpdl.mpg.de/imeji/collection/Kpsiw8PSKETsPdQV. Transgenic lines screened and used in this study are listed in *SI Appendix*, Table S2.

Predation Assay. The predation assay was performed in a field plantation at the WCCER, located in Arizona (34°55′17.8″N 112°50′42.2″W) in the summer of 2017. 3 RILs (generation F12) and 1 UT WT plant were grown in quadruplets at the corners of a 30 × 30-cm square. Quadruplets were separated by approximately 1 m. One set of plants of the entire AI-RIL population formed 1 block, and within each block, genotypes were randomly distributed; 4 blocks were planted ($n = 4$). Elongating plants were treated with wounding plus *M. sexta* regurgitant on 3 expanded rosette leaves 5 d before the predation assay and leaf discs were collected for unrelated analyses to be reported elsewhere. Six RILs with extreme differences in 6 terpenoid VOCs, UT-WT, and AZ-WT plants were used for the predation assay ($n = 4$). On the first morning of the assay, 1 *M. sexta* larva in the first instar was placed onto the adaxial side of the tip of the youngest rosette leaf and 3 *M. sexta* eggs were glued to the abaxial side of the same leaf. Larvae and eggs were counted as predated if they were completely empty and the remnant of the body or egg remained on the leaf. Predated larvae and eggs were counted at dusk, and missing (predated or lost from the plant for unclear reasons) larvae and eggs, and any which had dried out were replaced with new eggs and larvae. The second morning, predated larvae and eggs were counted a second time and all eggs and larvae were replaced. Counting was repeated at dusk and the following morning. The cumulative predation observed after 72 h is shown in Fig. 1*C*.

T-DNA Copy Number and Integrity Determination Using NanoString's nCounter Technology. T-DNA copy number and integrity were determined using either Southern blotting or NanoString's nCounter Technology. Genomic DNA from transgenic plant lines was isolated by a modified cetyl-trimethylammonium bromide method (63). For Southern blotting, the hptII_3 probe binding to the hygromycin phosphotransferase gene (66) was used after digestion of gDNA with either XbaI or EcoRI. For nCounter Technology, 5 μg of gDNA per sample was dissolved in water at a concentration of 30 ng/μL and sheared to fragment sizes mainly between 250 and 500 bp using a Covaris M220 Focused-ultrasonicator instrument according to the manufacturer's instructions. Sheared gDNA was precipitated, washed twice with 70% ethanol, and dissolved in water (12 μL). This DNA (1 μL) was used to confirm shearing on a 1% agarose gel.

For the nCounter analysis, a 12-code probe set (sequences in Dataset S1) was designed from of 12 target regions comprising 3 calibrator genes that occur as a single copy in the genome of *N. attenuata* and 9 functional regions indicative of complete T-DNA insertions or T-DNA overreads of the transformation vectors used for *N. attenuata* (*SI Appendix, Supplementary Information Text*). The oligonucleotides were designed by NanoString and synthesized by Integrated DNA technologies. The location of the target sequences on the binary plant transformation vectors is indicated in *SI Appendix*, Fig. S10*B*. Sheared gDNA (4 μL) was hybridized with the 12-code probe set and an XT-TagSet-12 according to NanoString's nCounter protocols and run together with a gDNA sample from a line known to have a complete single T-DNA insertion (previously confirmed by Southern blotting and nCounter) on a cartridge in an nCounter Sprint. The raw reads measured by the instrument were normalized as follows: the geometric mean of the 3 calibrator values for each of the 12 samples was calculated. The geometric mean of the 12 geometric means was calculated. The normalization factor for each sample was calculated by dividing the 12-sample geometric mean values by the geometric mean of each individual sample. For normalization, the value for each probe was multiplied with the normalization factor for the respective probe.

ACKNOWLEDGMENTS. This work was funded by the Max Planck Society and Advanced Grant 293926 of the European Research Council (to I.T.B.), and in part supported by the Collaborative Research Centre ChemBioSys (CRC 1127) funded by the Deutsche Forschungsgemeinschaft. We thank Prescott College, Northern Arizona University, the Arboretum at Flagstaff, Prescott National Forest, and the Southwest Experimental Garden Array for the use of a field plot at the Walnut Creek Center for Education and Research; the R. and N. Carlson and Southwest Experimental Garden Array staff for assistance with field plantations and the 2017 MPI-CE field team for assistance with sample collection for internal linalool measurements from field samples; Dr. B. S. Hansson for providing resources for moth breeding and wind tunnel assays; Dr. J. Gershenzon for providing resources for heterologous expression assays; Dr. E. Pichersky for providing plasmids with the *CbLIS* and *ObLIS* ORFs; A. Wissgott for plant transformation; Dr. D. Kessler for help with the tent experiments; Dr. Y. Oh and K. Pu for help with the GC-MS measurements; Dr. J. Li, Dr. H. Guo, Dr. Y. Zou, Dr. M. Wang, Dr. S. Li, and Dr. D. Li for daily discussion and critical comments in the laboratory; and Dr. S. Olsson and Dr. V. Pragadeesh for helpful discussions on linalool.

1. F. Loreto, M. Dicke, J. P. Schnitzler, T. C. J. Turlings, Plant volatiles and the environment. *Plant Cell Environ.* **37**, 1905–1908 (2014).
2. I. T. Baldwin, Plant volatiles. *Curr. Biol.* **20**, R392–R397 (2010).
3. A. Scala, S. Allmann, R. Mirabella, M. A. Haring, R. C. Schuurink, Green leaf volatiles: A plant's multifunctional weapon against herbivores and pathogens. *Int. J. Mol. Sci.* **14**, 17781–17811 (2013).
4. M. C. Schuman, N. Heinzel, E. Gaquerel, A. Svatos, I. T. Baldwin, Polymorphism in jasmonate signaling partially accounts for the variety of volatiles produced by *Nicotiana attenuata* plants in a native population. *New Phytol.* **183**, 1134–1148 (2009).
5. S. Allmann, I. T. Baldwin, Insects betray themselves in nature to predators by rapid isomerization of green leaf volatiles. *Science* **329**, 1075–1078 (2010).
6. K. Boonprab, K. Matsui, Y. Akakabe, N. Yotsukura, T. Kajiwara, Hydroperoxy-arachidonic acid mediated n-hexanal and (*Z*)-3- and (*E*)-2-nonenal formation in *Laminaria angustata*. *Phytochemistry* **63**, 669–678 (2003).
7. H. M. Chen *et al.*, A multifunctional lipoxygenase from *Pyropia haitanensis*-The cloned and functioned complex eukaryotic algae oxylipin pathway enzyme. *Algal Res.* **12**, 316–327 (2015).
8. F. Chen, D. Tholl, J. Bohlmann, E. Pichersky, The family of terpene synthases in plants: A mid-size family of genes for specialized metabolism that is highly diversified throughout the kingdom. *Plant J.* **66**, 212–229 (2011).
9. R. Halitschke, A. Keßler, J. Kahl, A. Lorenz, I. T. Baldwin, Ecophysiological comparison of direct and indirect defenses in *Nicotiana attenuata*. *Oecologia* **124**, 408–417 (2000).

10. T. Kuzuyama, H. Seto, Two distinct pathways for essential metabolic precursors for isoprenoid biosynthesis. *Proc. Jpn. Acad. Ser. B Phys. Biol. Sci.* **88**, 41–52 (2012).
11. J. K. Holopainen, J. Gershenzon, Multiple stress factors and the emission of plant VOCs. *Trends Plant Sci.* **15**, 176–184 (2010).
12. A. Kessler, I. T. Baldwin, Defensive function of herbivore-induced plant volatile emissions in nature. *Science* **291**, 2141–2144 (2001).
13. C. M. De Moraes, M. C. Mescher, J. H. Tumlinson, Caterpillar-induced nocturnal plant volatiles repel conspecific females. *Nature* **410**, 577–580 (2001).
14. R. A. Raguso More lessons from linalool: Insights gained from a ubiquitous floral volatile. *Curr. Opin. Plant Biol.* **32**, 31–36 (2016).
15. J. T. Knudsen, R. Eriksson, J. Gershenzon, B. Stahl, Diversity and distribution of floral scent. *Bot. Rev.* **72**, 1–120 (2006).
16. A. L. Parachnowitsch, R. C. Burdon, R. A. Raguso, A. Kessler, Natural selection on floral volatile production in *Penstemon digitalis*: Highlighting the role of linalool. *Plant Signal. Behav.* **8**, e22704 (2013).
17. J. F. Ginglinger *et al*., Gene coexpression analysis reveals complex metabolism of the monoterpene alcohol linalool in Arabidopsis flowers. *Plant Cell* **25**, 4640–4657 (2013).
18. V. S. Pragadheesh, C. S. Chanotiya, S. Rastogi, A. K. Shasany, Scent from *Jasminum grandiflorum* flowers: Investigation of the change in linalool enantiomers at various developmental stages using chemical and molecular methods. *Phytochemistry* **140**, 83–94 (2017).
19. R. Kaiser, The scent of orchids. Olfactory and chemical investigations. *Flavour Fragrance J.* **8**, 295 (1993).
20. J. T. Knudsen, L. Tollsten, Trends in floral scent chemistry in pollination syndromes—Floral scent composition in moth-pollinated taxa. *Bot. J. Linn. Soc.* **113**, 263–284 (1993).
21. J. A. Riffell, H. Lei, J. G. Hildebrand, Neural correlates of behavior in the moth *Manduca sexta* in response to complex odors. *Proc. Natl. Acad. Sci. U.S.A.* **106**, 19219–19226 (2009).
22. R. A. Raguso, E. Pichersky, New perspectives in pollination biology: Floral fragrances. A day in the life of a linalool molecule: Chemical communication in a plant-pollinator system. Part 1: Linalool biosynthesis in flowering plants. *Plant Species Biol.* **14**, 95–120 (1999).
23. C. E. Reisenman, J. A. Riffell, E. A. Bernays, J. G. Hildebrand, Antagonistic effects of floral scent in an insect-plant interaction. *Proc. Biol. Sci.* **277**, 2371–2379 (2010).
24. B. Boachon *et al*., CYP76C1 (Cytochrome P450)-mediated linalool metabolism and the formation of volatile and soluble linalool oxides in Arabidopsis flowers: A strategy for defense against floral antagonists. *Plant Cell* **27**, 2972–2990 (2015).
25. C. C. N. van Schie, M. A. Haring, R. C. Schuurink, Tomato linalool synthase is induced in trichomes by jasmonic acid. *Plant Mol. Biol.* **64**, 251–263 (2007).
26. J. S. Yuan *et al*., Elucidation of the genomic basis of indirect plant defense against insects. *Plant Signal. Behav.* **3**, 720–721 (2008).
27. J. S. Yuan *et al*., Molecular and genomic basis of volatile-mediated indirect defense against insects in rice. *Plant J.* **55**, 491–503 (2008).
28. Y. Du *et al*., Identification of semiochemicals released during Aphid feeding that attract parasitoid *Aphidius ervi*. *J. Chem. Ecol.* **24**, 1355–1368 (1998).
29. A. A. Rudmann, J. R. Aldrich, Chirality determinations for a tertiary alcohol—Ratios of linalool enantiomers in insects and plants. *J. Chromatogr. A* **407**, 324–329 (1987).
30. A. Giglio *et al*., The defensive secretion of *Carabus lefebvrei* Dejean 1826 pupa (Coleoptera, Carabidae): Gland ultrastructure and chemical identification. *Microsc. Res. Tech.* **72**, 351–361 (2009).
31. M. C. Lemfack *et al*., mVOC 2.0: A database of microbial volatiles. *Nucleic Acids Res.* **46**, D1261–D1265 (2018).
32. J. Wu, C. Hettenhausen, M. C. Schuman, I. T. Baldwin, A comparison of two *Nicotiana attenuata* accessions reveals large differences in signaling induced by oral secretions of the specialist herbivore *Manduca sexta*. *Plant Physiol.* **146**, 927–939 (2008).
33. A. Steppuhn, M. C. Schuman, I. T. Baldwin, Silencing jasmonate signalling and jasmonate-mediated defences reveals different survival strategies between two *Nicotiana attenuata* accessions. *Mol. Ecol.* **17**, 3717–3732 (2008).
34. W. Zhou *et al*., Tissue-specific emission of (*E*)-α-bergamotene helps resolve the dilemma when pollinators are also herbivores. *Curr. Biol.* **27**, 1336–1341 (2017).
35. M. C. Schuman, D. Kessler, I. T. Baldwin, Ecological observations of native *Geocoris pallens* and *G. punctipes* populations in the Great Basin Desert of Southwestern Utah. *Psyche (Camb., Mass.)* **2013**, 465108 (2013).
36. S. Xu *et al*., Wild tobacco genomes reveal the evolution of nicotine biosynthesis. *Proc. Natl. Acad. Sci. U.S.A.* **114**, 6133–6138 (2017).
37. K. Gase, Nicotiana attenuata strain UT unplaced genomic scaffold, NIATTr2, whole genome shotgun sequence. *GenBank*. https://www.ncbi.nlm.nih.gov/nuccore/NW_017670477.1. Deposited 15 November 2016.
38. K. Gase, Nicotiana attenuata strain UT chromosome 11, NIATTr2, whole genome shotgun sequence. *Genbank*. https://www.ncbi.nlm.nih.gov/nuccore/NC_031999.1. Deposited 15 November 2016.
39. T. Brockmöller *et al*., *Nicotiana attenuata* data hub (NaDH): An integrative platform for exploring genomic, transcriptomic and metabolomic data in wild tobacco. *BMC Genomics* **18**, 79 (2017).
40. C. Hettenhausen, I. T. Baldwin, J. Wu, Silencing *MPK4* in *Nicotiana attenuata* enhances photosynthesis and seed production but compromises abscisic acid-induced stomatal closure and guard cell-mediated resistance to *Pseudomonas syringae* pv tomato DC3000. *Plant Physiol.* **158**, 759–776 (2012).
41. C. E. Reisenman, T. A. Christensen, W. Francke, J. G. Hildebrand, Enantioselectivity of projection neurons innervating identified olfactory glomeruli. *J. Neurosci.* **24**, 2602–2611 (2004).
42. S. Bisch-Knaden, A. Dahake, S. Sachse, M. Knaden, B. S. Hansson, Spatial representation of feeding and oviposition odors in the brain of a hawkmoth. *Cell Rep.* **22**, 2482–2492 (2018).
43. N. Dudareva, L. Cseke, V. M. Blanc, E. Pichersky, Evolution of floral scent in *Clarkia*: Novel patterns of S-linalool synthase gene expression in the *C. breweri* flower. *Plant Cell* **8**, 1137–1148 (1996).
44. Y. Iijima *et al*., The biochemical and molecular basis for the divergent patterns in the biosynthesis of terpenes and phenylpropenes in the peltate glands of three cultivars of basil. *Plant Physiol.* **136**, 3724–3736 (2004).
45. D. Kessler *et al*., How scent and nectar influence floral antagonists and mutualists. *eLife* **4**, e07641 (2015).
46. A. Aharoni *et al*., Terpenoid metabolism in wild-type and transgenic Arabidopsis plants. *Plant Cell* **15**, 2866–2884 (2003).
47. T. Yang, G. Stoopen, M. Thoen, G. Wiegers, M. A. Jongsma, *Chrysanthemum* expressing a linalool synthase gene 'smells good', but 'tastes bad' to Western flower thrips. *Plant Biotechnol. J.* **11**, 875–882 (2013).
48. J. Lücker, *et al*., Expression of *Clarkia* S-linalool synthase in transgenic petunia plants results in the accumulation of S-linalyl-β-D-glucopyranoside. *Plant J.* **27**, 315–324 (2001).
49. M. C. Schuman, E. C. Palmer-Young, A. Schmidt, J. Gershenzon, I. T. Baldwin, Ectopic terpene synthase expression enhances sesquiterpene emission in *Nicotiana attenuata* without altering defense or development of transgenic plants or neighbors. *Plant Physiol.* **166**, 779–797 (2014).
50. N. Dudareva *et al*., (*E*)-β-ocimene and myrcene synthase genes of floral scent biosynthesis in snapdragon: Function and expression of three terpene synthase genes of a new terpene synthase subfamily. *Plant Cell* **15**, 1227–1241 (2003).
51. F. Chen *et al*., Biosynthesis and emission of terpenoid volatiles from Arabidopsis flowers. *Plant Cell* **15**, 481–494 (2003).
52. A. Aharoni *et al*., Gain and loss of fruit flavor compounds produced by wild and cultivated strawberry species. *Plant Cell* **16**, 3110–3131 (2004).
53. V. Falara *et al*., The tomato terpene synthase gene family. *Plant Physiol.* **157**, 770–789 (2011).
54. X. Z. Huang *et al*., The terpene synthase gene family in *Gossypium hirsutum* harbors a linalool synthase GhTPS12 implicated in direct defence responses against herbivores. *Plant Cell Environ.* (2017).
55. A. K. BorgKarlson, C. R. Unelius, I. Valterova, L. A. Nilsson, Floral fragrance chemistry in the early flowering shrub *Daphne mezereum*. *Phytochemistry* **41**, 1477–1483 (1996).
56. R. R. Junker, J. Gershenzon, S. B. Unsicker, Floral odor bouquet loses its ant repellent properties after inhibition of terpene biosynthesis. *J. Chem. Ecol.* **37**, 1323–1331 (2011).
57. E. H. Koschier, W. J. De Kogel, J. H. Visser, Assessing the attractiveness of volatile plant compounds to Western flower thrips *Frankliniella occidentalis*. *J. Chem. Ecol.* **26**, 2643–2655 (2000).
58. E. J. McCallum *et al*., Increased plant volatile production affects oviposition, but not larval development, in the moth *Helicoverpa armigera*. *J. Exp. Biol.* **214**, 3672–3677 (2011).
59. Y. Xiao *et al*., Specific herbivore-induced volatiles defend plants and determine insect community composition in the field. *Ecol. Lett.* **15**, 1130–1139 (2012).
60. A. Haverkamp, B. S. Hansson, M. Knaden, Combinatorial codes and labeled lines: How insects use olfactory cues to find and judge food, mates, and oviposition sites in complex environments. *Front. Physiol.* **9**, 49 (2018).
61. J. N. Thompson, Specific hypotheses on the geographic mosaic of coevolution. *Am. Nat.* **153**, S1–S14 (1999).
62. A. C. Aprotosoaie, M. Hancianu, I. I. Costache, A. Miron, Linalool: A review on a key odorant molecule with valuable biological properties. *Flavour Fragrance J.* **29**, 193–219 (2014).
63. J. H. Loughrin, D. A. Potter, T. R. Hamilton-Kemp, Volatile compounds induced by herbivory act as aggregation kairomones for the Japanese beetle (Popillia japonica Newman). *J. Chem. Ecol.* **21**, 1457–1467 (1995).
64. T. C. J. Turlings *et al*., How caterpillar-damaged plants protect themselves by attracting parasitic wasps. *Proc. Natl. Acad. Sci. U.S.A.* **92**, 4169–4174 (1995).
65. B. Bubner, K. Gase, I. T. Baldwin, Two-fold differences are the detection limit for determining transgene copy numbers in plants by real-time PCR. *BMC Biotechnol.* **4**, 14 (2004).
66. K. Gase, A. Weinhold, T. Bozorov, S. Schuck, I. T. Baldwin, Efficient screening of transgenic plant lines for ecological research. *Mol. Ecol. Resour.* **11**, 890–902 (2011).